Thermodynamics and kinetics of competing aggregation processes in a simple model system

Ambarish Nag[a] and R. Stephen Berry[b]
Department of Chemistry, The University of Chicago, 5640 South Ellis Avenue, Chicago, Illinois 60637, USA and The James Franck Institute, The University of Chicago, 5640 South Ellis Avenue, Chicago, Illinois 60637, USA

(Received 15 December 2006; accepted 7 August 2007; published online 8 November 2007)

A simple model system has been used to develop thermodynamics and kinetics for bulk and surface aggregation processes capable of competing with each other. The processes are the stepwise aggregation of monomers in a fluid medium and on an inpenetrable solid surface bounding the fluid medium, besides the adsorption and desorption of the same species at the solid-fluid interface. Emphasis is on aggregation processes in the high friction limit. The theoretical model is used to compare the kinetics and thermodynamics of the processes and to infer the conditions in which one process dominates another, in the high friction limit, such as in a liquid. The motivation of this study is obtaining insight into competition between aggregation in solution and on an adjoining surface, such as a cell membrane. © *2007 American Institute of Physics*. [DOI: 10.1063/1.2777137]

I. INTRODUCTION

Aggregation processes are ubiquitous in chemistry and biology. Many aggregation processes, of considerable chemical or biological significance, are facilitated by surfaces.[1–5] Most real life surface aggregation processes are so complex that it is prohibitively difficult to model such systems theoretically from fundamental statistical mechanics and reaction rate theories. However, simple model systems can be designed, for which the aggregation rates and equilibrium constants can be calculated theoretically, with considerable rigor. Understanding the kinetics and thermodynamics of such simple systems can be a good starting point for theoretical modeling of more complex interfacial aggregation systems.

This article deals with such a simple model system. In this system, a number of aggregation processes occur between identical spherical monomers suspended in solution or adsorbed at a surface. The monomers interact with each other via a pairwise attractive Sutherland-type potential,[6] and with the surface through a generalized Lennard-Jones potential. We assume that these monomers aggregate to form only rigid rod (inflexible chain)like structures which grow only at either end. Under these assumptions, expressions can be obtained for the rates at which a single monomer aggregates with or dissociates from another single monomer or a rodlike aggregate in solution or on the surface. Besides, the rate at which a single monomer adsorbs on or desorbs from the surface can be evaluated. It is also relatively straightforward to calculate equilibrium constants for the aggregation equilibria. In the current article, physically important ratios of these rates and equilibrium constants are calculated as a function of three parameters, viz., intermonomer binding energy, monomer-surface binding energy and size (diameter) of each monomer. Comparison of these rates and equilibrium constants over physically relevant parameter regimes indicates conditions under which the solution and surface aggregation processes compete with each other. Such a comparison also provides a method of enhancing one process over the other by tuning some or all of the parameters. Thus, this model can be used to explain quantitatively how the presence of a surface can boost the aggregation rate over that in solution.

The expressions for the rates and equilibrium constants are first obtained for a system containing only monomers and dimers. These results are then extended to include formation of larger aggregates. Most of the equations and results discussed in this paper pertain to a high friction fluid. Some equations for a low friction fluid are discussed in the supplementary information.[7]

It should be emphasized that our aim in this article is to develop a methodological approach for modeling aggregation processes rather than to model any particular biological or chemical system. Supplementary information is available regarding the equilibrium and rate coefficients in both the high friction limit treated here and the low friction limit, and regarding one useful substitution introduced below.[7]

II. THE SYSTEM AND SOME DEFINITIONS

Reactions involving equilibria of a number of species are considered here. There are isolated spherical monomers suspended in a high friction fluid (solution) medium, or adsorbed at the surface of the solution with a flat impermeable surface. These spherical monomers form rodlike (inflexible chain) aggregates of different lengths, either in solution or on the surface. The isolated monomers in solution are denoted by B_f and those adsorbed at the surface by B_i. Aggregates of

[a]Current address: Theoretical Biology and Biophysics Group, Los Alamos National Laboratory, Los Alamos, New Mexico 87545, U.S.A. Electronic mail: ambarish@lanl.gov
[b]Author to whom correspondence should be addressed. Electronic mail: berry@uchicago.edu

size n in solution and adsorbed at the surface are denoted by B_{fn} and B_{in}, respectively. The system is enclosed in a cube of volume L^3 in the fluid medium and the bottom face of the cube represents the surface.

The volume of the cube is assumed to be so large, compared to the monomer and aggregate sizes, that the boundary effects on monomers and aggregates at the bottom surface can be studied without taking into account the boundary effects due to the other faces of the cube. Thus, no aggregate in our model can cause critical inhomogenity within the reaction volume by approaching its size. These assumptions are reasonable in light of the fact that we endeavor to model aggregation phenomena in the vicinity of a surface where the size of the aggregates is much smaller than the extension of the surface or of the reaction compartment adjacent to the surface.

The solvent molecules constitute the heat bath at temperature T. We assume that the spatial distributions of both the solution and surface species are uniform. The reactions under consideration are

$$2B_f \rightleftharpoons B_{f2}; \quad B_{f2} + B_f \rightleftharpoons B_{f3}; \quad \cdots \quad B_{f(n-1)} + B_f \rightleftharpoons B_{fn};$$

$$2B_i \rightleftharpoons B_{i2}; \quad B_{i2} + B_i \rightleftharpoons B_{i3}; \quad \cdots \quad B_{i(n-1)} + B_i \rightleftharpoons B_{fn};$$

$$B_f \rightleftharpoons B_i; \quad B_{f2} \rightleftharpoons B_{i2}; \quad \cdots \quad B_{fn} \rightleftharpoons B_{in}. \tag{1}$$

In our model, the rodlike aggregates can grow only by adding monomers at either end of the rod. A set of equilibrium constants can be defined in terms of the fraction of the total number of elementary monomers present.

$$\mathrm{Kp}_{12}^{(3d)} = \alpha_{f2}/\alpha_f^2; \quad \mathrm{Kp}_{23}^{(3d)} = \alpha_{f3}/\alpha_{f2}\alpha_f; \quad \cdots \quad \mathrm{Kp}_{(n-1)n}^{(3d)} = \alpha_{fn}/\alpha_{f(n-1)}\alpha_f;$$

$$\mathrm{Kp}_{12}^{(2d)} = \alpha_{i2}/\alpha_i^2; \quad \mathrm{Kp}_{23}^{(2d)} = \alpha_{i3}/\alpha_{i2}\alpha_i; \quad \cdots \quad \mathrm{Kp}_{(n-1)n}^{(2d)} = \alpha_{in}/\alpha_{i(n-1)}\alpha_i; \tag{2}$$

$$\mathrm{Kp}^{ps} = \alpha_i/\alpha_f. \tag{3}$$

These equilibrium constants are henceforth referred to as the fractional equilibrium constants. The fractional equilibrium constant for formation of an aggregate of n monomers, from one comprising $(n-1)$ monomer(s), is denoted by $\mathrm{Kp}_{(n-1)n}$. In the above equations, α_k denotes the fraction of the total number of monomers present as the kth species. It can be shown that the corresponding concentration equilibrium constants K_{eq} can be related to the fractional equilibrium constants Kp by the relations

$$\mathrm{Kp}_{(n-1)n}^{(3d)} = \frac{n}{(n-1)} K_{\mathrm{eq}(n-1)n}^{(3d)} [B]_{\mathrm{tot}},$$

$$\mathrm{Kp}_{(n-1)n}^{(2d)} = \frac{n}{(n-1)} K_{\mathrm{eq}(n-1)n}^{(2d)} L[B]_{\mathrm{tot}},$$

$$\mathrm{Kp}^{ps} = \frac{K_{\mathrm{eq}}^{ps}}{L}. \tag{4}$$

The total concentration of the monomers, present in all forms, is denoted by $[B]_{\mathrm{tot}}$. The fractions of the total number of monomers, present as different species, obey the constraint

$$\alpha_f + \alpha_i + \alpha_{f2} + \alpha_{i2} + \cdots + \alpha_{f(n-1)} + \alpha_{i(n-1)} + \alpha_{fn} + \alpha_{in} = 1. \tag{5}$$

By substituting all α's in terms of α_f and the fractional equilibrium constants, one obtains

$$\begin{aligned}
&(\mathrm{Kp}_{12}^{(3d)}\mathrm{Kp}_{23}^{(3d)} \cdots \mathrm{Kp}_{(n-1)n}^{(3d)} \\
&\quad + (\mathrm{Kp}^{ps})^n \mathrm{Kp}_{12}^{(2d)}\mathrm{Kp}_{23}^{(2d)} \cdots \mathrm{Kp}_{(n-1)n}^{(2d)})\alpha_f^n \\
&\quad + (\mathrm{Kp}_{12}^{(3d)}\mathrm{Kp}_{23}^{(3d)} \cdots \mathrm{Kp}_{(n-2)(n-1)}^{(3d)} \\
&\quad + (\mathrm{Kp}^{ps})^{n-1} \mathrm{Kp}_{12}^{(2d)}\mathrm{Kp}_{23}^{(2d)} \cdots \mathrm{Kp}_{(n-2)(n-1)}^{(2d)})\alpha_f^{n-1} + \cdots \\
&\quad + (\mathrm{Kp}_{12}^{(3d)} + (\mathrm{Kp}^{ps})^2 \mathrm{Kp}_{12}^{(2d)})\alpha_f^2 + (1 + \mathrm{Kp}^{ps})\alpha_f - 1.0 = 0.0.
\end{aligned} \tag{6}$$

The value of α_f is obtained by solving the above equation. Once α_f is calculated, all the concentrations can be obtained in terms of $[B]_{\mathrm{tot}}$. The fact that the Kp's are especially convenient for determining α_f is the main reason for formulating the problem in terms of Kp's rather than of the concentration equilibrium constants.

III. THEORY

A. Monomer-monomer association

We consider two monomers, labeled as A and B, coupled to a fluid bath via fluctuating random forces characterized by friction coefficients, ζ_{A} and ζ_{B}. Because of the great disparity in size of the reaction volume and the monomer in our model, we can neglect boundary effects due to the finite size of the reaction volume on the diffusive motion of the monomers in solution for all practical purposes. Hence, in our model, it is reasonable to relate the friction coefficients ζ_{A} and ζ_{B} to the translational diffusion coefficients D_{A} and D_{B}, respectively, by the Einstein relation,

$$D = \frac{kT}{\zeta}, \tag{7}$$

where k is the Boltzmann constant.

The two monomers interact with each other via a direct interaction potential $V(R)$. The friction coefficient ζ_{A} of monomer A and ζ_{B} of monomer B are assumed to be space and time invariant. It has been shown by Rodger and Sceats[8,9] that the Fokker-Planck equation (FPE) for an interacting pair of monomers, A and B, can be reduced to an FPE

in one dimension, describing the motion of a single particle with effective mass μ_{AB} (the reduced mass of monomers A and B), and effective friction coefficient ζ_{eff}, over an effective potential given by

$$\tilde{V}(R) = V(R) - 2kT \ln R \tag{8}$$

where the R in the logarithm is the intermonomer separation divided by 1 Å. The effective friction coefficient for the pair of monomers is given by

$$\zeta_{eff} = \left(\frac{m_B}{M}\right)^2 \zeta_A + \left(\frac{m_A}{M}\right)^2 \zeta_B, \tag{9}$$

where m_A and m_B are the respective masses of A and B, and $M = m_A + m_B$. The important assumptions involved in obtaining the effective potential and friction coefficient are that the center of mass coordinates and the rotational degrees of freedom are thermalized, as is usually the case.

The effective diffusion coefficient D_{eff} for the monomer pair is defined as

$$D_{eff} = \frac{kT}{\zeta_{eff}}, \tag{10}$$

which, in general, is not the same as the relative diffusion coefficient of the monomer pair D_r, given by

$$D_r = D_A + D_B = kT \frac{\zeta_A \zeta_B}{\zeta_A + \zeta_B}. \tag{11}$$

In the limit that the two aggregating monomers are identical, $m_A = m_B$ and $\zeta_A = \zeta_B = \zeta$, Eq. (9) reduces to

$$\zeta_{eff} = \frac{\zeta}{2}, \tag{12}$$

and D_{eff} turns out to be the same as D_r.

Following closely in the footsteps of Rodger and Sceats,[8,9] Dawes and Sceats[10] have reduced the FPE of the system of a pair of interacting monomers restricted to a surface to an FPE describing the motion of a single monomer having the reduced mass of the two-monomer system, with an effective friction coefficient given by Eq. (9), moving over an effective one-dimensional potential given by

$$\tilde{V}(R) = V(R) - kT \ln R. \tag{13}$$

All the other degrees of freedom of the system other than the intermonomer distance are assumed to be in thermal equilibrium, including those describing the binding of the monomers to the surface.

When the direct interaction potential $V(R)$ between the two monomers is sufficiently attractive, the resulting effective potential $\tilde{V}(R)$ exhibits a transition state (say at R_T) because of the repulsive character of the logarithmic entropic term. This term accounts for the increase in configuration space as R increases and ensures that the one-dimensional equilibrium distribution $e^{[-\tilde{V}(R)/kT]}$ mimics the exact three dimensional distribution $R^2 e^{[-V(R)/kT]}$ for the two interacting monomers in solution, and the correct two-dimensional distribution $Re^{[-V(R)/kT]}$ for the two monomers restricted to a surface. The inner minimum is at R_p, the internuclear distance of the dimer; if $R < R_T$, the monomers are combined, and if $R > R_T$, they are dissociated. Encounter of the two monomers is defined to occur when successful crossing at R_T to the R_p side occurs. Whether or not successful reaction occurs depends on whether a successful encounter is followed by thermalization in the vicinity of R_p.[9] In this article, the probability of this thermalization is always set to unity.

Thus, the dynamics of the two monomers is reduced by the Rodger-Sceats scheme into barrier crossing dynamics of a single particle, having the reduced mass of the two monomers over an effective one-dimensional potential with an effective friction. Then, Kramers' solution[11,12] can be applied to this one-dimensional barrier crossing problem.

In order to determine the equilibrium constants and second order rate coefficients for dimerization in solution and on the surface, the first step is to consider a spherical volume (solution case), or a circular area (surface case), of radius R_c around a monomer A, which equals the mean intermonomer separation in solution or on the surface. This sphere (circle) should contain only another monomer B, and this constraint is implemented by setting $V(R_c) = \infty$ for $R > R_c$. This causes $\tilde{V}(R)$ to adopt a double well form, with the inner minimum located at R_p and the outer one at R_c, with the barrier between the two minima occurring at R_T. The barrier crossing dynamics is characterized by the dissociation attempt frequency ω_p and the barrier crossing frequency ω_T. They are defined as[9]

$$\omega_p = \frac{(2\pi kT/\mu_{AB})^{1/2}}{\int_{R_p}^{R_T} dR e^{-[\tilde{V}(R) - \tilde{V}(R_p)]/kT}} \tag{14}$$

and

$$\omega_T = \frac{(2\pi kT/\mu_{AB})^{1/2}}{\int_{R_p}^{R_c} dR e^{[\tilde{V}(R) - \tilde{V}(R_T)]/kT}}. \tag{15}$$

An equilibrium constant K_{eq}^{v} between bound and unbound forms of a pair of monomers, restricted to a sphere (circle) of radius R_c, can be defined in two ways.[10] It can be defined as the ratio of k_R to k_E, where the recombination rate k_R is the rate of crossing the barrier at R_T from $R > R_T$, and the escape rate k_E is the rate of escape from the potential well at R_p over the barrier at R_T. The equilibrium constant can also be defined in terms of partition functions, i.e., by using the unique partitioning of the the one-dimensional configuration space afforded by the transition state. The escape rate k_E can be determined from Kramers' theory.[11,12] The recombination rate k_R can be obtained from the expressions for k_E and the thermodynamic definition of the equilibrium constant K_{eq}^{v}. This k_R can be used to determine the corresponding second order rate coefficients,[10] which, in turn, are used to derive the expressions for the equilibrium constants involving the uniform macroscopic equilibrium concentrations of monomers and dimers in the macroscopic volume or surface area. The details of these derivations are provided in the supplementary information.[7]

Thus following along the lines of Dawes and Sceats,[10] it can be shown that

$$k_{2d}^{(2)}(\text{high friction}) = \frac{2\pi D_{\text{eff}}}{\sigma_s}\left(\frac{2\pi kT}{\mu_{\text{AB}}}\right)^{-1/2} R_{T2}\omega_T^{(2d)} e^{-[V(R_{T2})/kT]}. \tag{16}$$

Similarly, it can be shown that

$$k_{3d}^{(2)}(\text{high friction}) = \frac{4\pi D_{\text{eff}}}{\sigma_s}\left(\frac{2\pi kT}{\mu_{\text{AB}}}\right)^{-1/2} (R_{T3})^2\omega_T^{(3d)} e^{[-V(R_{T3})/kT]}, \tag{17}$$

where the subscripts $2d$ and $3d$ refer to the surface and solution cases respectively, superscript 2 indicates second-order, and the effective diffusion coefficient is given by D_{eff}. If A and B are identical, the symmetry number (σ_s) is 2. If the associating species are not identical and, hence, distinguishable from each other, the symmetry number is unity.

B. Rate coefficients and equilibrium constants for attractive Sutherland-type direct interaction potential between monomers

Next, we convert the general expressions for the equilibrium constants and second order rate coefficients for an arbitrary intermonomer potential $V(R)$ into more useful forms by using an attractive Sutherland form of the potential,[13] given by

$$V(R) = \begin{cases} -\epsilon_1(\sigma/R)^n, & R > \sigma \\ \infty, & R < \sigma, \end{cases} \tag{18}$$

where n is an integer, and $\sigma \equiv R_p$ is the position of the minimum of $V(R)$, so that ϵ_1 is the intermonomer binding energy. The value of n is chosen to be 6 so that the interaction between monomers corresponds to attractive dispersion interaction. It is assumed that the direct interaction potential $V(R)$, and hence ϵ_1, is the same in solution and on the surface, which is tantamount to neglecting the effects of surface corrugation and localization on the direct interaction potential for the surface case. It can be shown that the transition state of the effective potential in solution [Eq. (8)] occurs at

$$R_{T3} = \sigma\left(\frac{n\epsilon_1}{2kT}\right)^{1/n}, \tag{19}$$

and that of the effective potential on the surface [Eq. (13)] at

$$R_{T2} = \sigma\left(\frac{n\epsilon_1}{kT}\right)^{1/n}. \tag{20}$$

For the attractive Sutherland form of the intermonomer potential [Eq. (18)], Eq. (15) yields the following expressions for the barrier crossing frequencies in the surface and solution cases:

$$\omega_T^{(2d)} = \frac{(2\pi kT/\mu_{\text{AB}})^{1/2} e^{-1/n}}{R_{T2}\int_\sigma^{\text{Rc}_2} dR \frac{1}{R} e^{-(\epsilon_1/kT)(\sigma/R)^n}}, \tag{21}$$

$$\omega_T^{(3d)} = \frac{(2\pi kT/\mu_{\text{AB}})^{1/2} e^{-2/n}}{(R_{T3})^2\int_\sigma^{\text{Rc}_3} dR \frac{1}{R^2} e^{-\epsilon_1/kT(\sigma/R)^n}}. \tag{22}$$

On substituting the appropriate R_T from Eqs. (19) and (20), and the appropriate ω_T from Eqs. (21) and (22) into Eqs. (16) and (17), one obtains the following expressions for $k_{2d}^{(2)}$ and $k_{3d}^{(2)}$ in the high friction limit:

$$k_{2d}^{(2)}(\text{high friction}) = \frac{2\pi D_{\text{eff}}}{\sigma_s}\left[\int_\sigma^{\text{Rc}_2} dR \frac{1}{R} e^{-(\epsilon_1/kT)(\sigma/R)^n}\right]^{-1}, \tag{23}$$

$$k_{3d}^{(2)}(\text{high friction}) = \frac{4\pi D_{\text{eff}}}{\sigma_s}\left[\int_\sigma^{\text{Rc}_3} dR \frac{1}{R^2} e^{-(\epsilon_1/kT)(\sigma/R)^n}\right]^{-1}, \tag{24}$$

where Rc_2 and Rc_3 refer to the mean separation of the aggregating species on the surface and in solution, respectively. It should be noted that in our model, apart from the explicit dependence of the aggregation rates on the concentrations of the aggregating species, there is also an implicit concentration dependence via the Rc_3 and Rc_2 terms in the second order rate coefficients.

As outlined in the supplementary information,[7] the surface and solution association equilibrium constants are obtained as

$$K_{\text{eq12}}^{(2d)} = \frac{2\pi}{\sigma_s}\int_\sigma^{\sigma(n\epsilon_1/kT)^{1/n}} dRR e^{(\epsilon_1/kT)(\sigma/R)^n}, \tag{25}$$

$$K_{\text{eq12}}^{(3d)} = \frac{4\pi}{\sigma_s}\int_\sigma^{\sigma(n\epsilon_1/2kT)^{1/n}} dRR^2 e^{(\epsilon_1/kT)(\sigma/R)^n}. \tag{26}$$

The symmetry number σ_s is assigned the value of 2 in all of the above equations, as any monomer is indistinguishable from another.

To obtain the second order rate coefficients for formation of aggregates larger than dimers, we make the following assumptions. We assume that a dimer could add a third monomer on the same total cross section as in the monomer to dimer case. The concept here is that of a hemisphere of available area on each member of the dimer, in the solution case, and a semicircle around each member of the dimer adsorbed at the surface. However, the effective diffusion coefficient should differ from the monomer to the dimer case and a symmetry number σ_s of unity should be used because the two aggregating species are not identical.

In case of aggregation of a monomer B with an n-mer A ($n > 1$), Eqs. (9) and (10) yield the following effective diffusion coefficient:

$$\frac{1}{D_{\text{eff}}} = \left(\frac{1}{n+1}\right)^2\frac{1}{D_{\text{A}}} + \left(\frac{n}{n+1}\right)^2\frac{1}{D_{\text{B}}}. \tag{27}$$

For a rod shaped n-mer A, the orientationally averaged diffusion coefficient is expressed as[14]

$$D_A = \frac{k_B T(\ln(p) + \gamma)}{A\pi\eta L}, \tag{28}$$

where L is the rod length, $p = L/\sigma$ where σ is the diameter of the rod, $\gamma = 0.312 + 0.565/p + 0.10/p^2$, and $A = 3$.

Moreover, the Rc_2 and Rc_3 terms in the integrals, which refer to the mean separation between the aggregating species on the surface and in solution, respectively, vary with the size of the aggregate with which a monomer associates. For the association of two monomers to form a dimer, Rc_2 and Rc_3 are the mean distances between two monomers on the surface and in solution, respectively. Similarly, for the association of an n-mer with a monomer, the corresponding Rc_2 and Rc_3 values would be the mean separation between n-mers and monomers, on the surface and in solution, respectively.

By virtue of the above assumption that an n-mer would add another monomer with the same total cross section as in dimerization, we can also use Eqs. (25) and (26) for the formation of larger aggregates. However, for these cases, a symmetry number (σ_s) of unity should be used since the two aggregating species would not be identical. Thus,

$$K_{eq23}^{(2d)} = K_{eq34}^{(2d)} = 2\pi \int_{\sigma}^{\sigma(n\epsilon_1/kT)^{1/n}} dRRe^{(\epsilon_1/kT)(\sigma/R)^n}, \tag{29}$$

$$K_{eq23}^{(3d)} = K_{eq34}^{(3d)} = 4\pi \int_{\sigma}^{\sigma(n\epsilon_1/2kT)^{1/n}} dRR^2 e^{(\epsilon_1/kT)(\sigma/R)^n}. \tag{30}$$

C. Monomer adsorption and desorption

We assume that the interaction between a flat surface and a monomer is of the generalized Lennard-Jones form; the monomer-surface distance is given by the z coordinate. Once the monomer reaches the potential well region, it just rolls down the potential well, i.e., it gets adsorbed at the surface. Thus the rate of association of the monomers with the surface is dictated by the rate at which the monomers reach the surface. For the high friction limit, this is the problem of diffusion in one dimension to an absorbing wall. In order to find out how many monomers reach the surface per unit time from the continuum liquid, one needs to determine the probability that a monomer, starting at time $t=0$ from $z=0$ at a distance ξ from an absorbing wall located at $z=\xi$, will reach the wall for the first time at time t. Thus, what is needed is the first passage time distribution for a monomer starting at $z=0$ at time $t=0$ to arrive at $z=\xi$ with the initial condition $p(z=0,0)=\delta(z=0)$ and the absorbing boundary condition $p(\xi,t)=0$, where $p(z,t)$ is the probability of finding the monomer at z at time t. As shown in Appendix A, this first passage time distribution is given by

$$f(\xi,t) = \frac{\xi}{\sqrt{4\pi D t^3}} e^{-\xi^2/4Dt}, \tag{31}$$

where D is the diffusion coefficient of the monomer in the continuum liquid.

In this development, the system is bounded by a cubic box of volume L^3, the bottom face of which is the absorbing wall. The uniform equilibrium concentration $[B_f]$ of single monomers in solution is given the shorthand notation c. All the monomers in the infinitesimal element of the reaction volume, enclosed between the planes of area L^2 at $z=\xi$ and $z=\xi+d\xi$, can be taken to be at a distance ξ from the absorbing wall, for all practical purposes. The number of monomers in this volume element that reach the absorbing wall, for the first time in time t, is given by the product of the number of monomers in this volume element and the probability that a monomer in this volume element reaches the absorbing wall, for the first time, in time t. This product is $cL^2 d\xi f(\xi,t)$. Therefore, the total number of monomers reaching the surface area L^2 per unit time is obtained by integrating $cL^2 d\xi f(\xi, t=1)$ over the length of the box in the z direction, yielding $cL^2\sqrt{D/\pi}[1-e^{-L^2/4D}]$ as the number of monomers that reach the bottom face of the box per unit time. Therefore, the rate constant for the monomer adsorption in the diffusion regime is given by

$$k_{ps}^{(f)} = \sqrt{\frac{D}{\pi}}[1 - e^{-L^2/4D}]. \tag{32}$$

The above equation can also be used for the rate constant of a small cylindrical aggregate by replacing the diffusion coefficient of a single monomer (sphere) by the diffusion coefficient of the aggregate (cylinder) using Eq. (28).

The dissociation rate of an adsorbed monomer is next evaluated following the work of Larson and Lightfoot.[15] The potential for the monomer-surface interaction is assigned the generalized Lennard-Jones form,

$$V(z) = 4\epsilon_{ps}\left[\left(\frac{\sigma}{z}\right)^{2n_1} - \left(\frac{\sigma}{z}\right)^{n_1}\right], \tag{33}$$

where $n_1 = 4$ (see Appendix B) and z is the distance of the monomer from the surface at $z=0$. The generalized Lennard-Jones diameter is the same as for the attractive Sutherland-type direct interaction potential between monomers.

In the intermediate to high friction regime, monomer motion is diffusive, and escape of the the adsorbed monomer from the surface can only be defined as the attainment of a certain arbitrary distance from the bottom of the monomer-surface potential well. Evidently, Kramers' theory is not applicable to this situation, since a barrier curvature cannot be defined. Because the generalized Lennard-Jones potential is only one dimensional, one cannot define an entropic contribution from it that gives rise to a barrier. The problem of escape of a monomer from the well, in the diffusion controlled regime, has been dealt with by Larson and Lightfoot.[15] They chose a cutoff (escape) location where the potential is nearly flat. For such a choice of the escape point given by $L_c\sigma$, it can be shown, starting from the Smoluchowski equation, that the escape rate constant from the surface is

$$k_{ps}^{(b)} = \left(\frac{kT}{2\pi m}\right)^{1/2} \frac{m}{\zeta\sigma} \frac{(\epsilon_{ps}/m)^{1/2}(n_1/\sigma)2^{1/2-1/n_1}e^{-\epsilon_{ps}/kT}}{[L_c - (4\epsilon_{ps}/kT)^{1/n_1}\Gamma(1-1/n_1)]}, \tag{34}$$

where m is the monomer mass. The above equation for $k_{ps}^{(b)}$ has been obtained by Larson and Lightfoot[15] for the conditions that

$$\frac{\epsilon_{ps}/kT}{L_c^{n_1}} \ll 1, \tag{35}$$

so that the potential is nearly flat at the cutoff point, and

$$e^{\epsilon_{ps}/kT}\sqrt{\frac{kT}{\epsilon_{ps}}} \gg L_c. \tag{36}$$

Inequality (36) demands that we cannot consider a very small value of ϵ_{ps}/kT. If L_c is taken as 10, and the range of ϵ_{ps}/kT is 10–100, then both the above inequalities are satisfied. Hence, in all the calculations in this paper, the smallest value of ϵ_{ps}/kT and L_c are both taken to be 10.

Substitution of ζ from Eq. (7) in Eq. (34) yields

$$k_{ps}^{(b)} = \frac{D}{(2\pi kT)^{1/2}\sigma}\frac{(\epsilon_{ps})^{1/2}(n_1/\sigma)2^{1/2-1/n_1}e^{-\epsilon_{ps}/kT}}{[L_c-(4\epsilon_{ps}/kT)^{1/n_1}\Gamma(1-1/n_1)]}. \tag{37}$$

The expressions for $k_{ps}^{(f)}$ and $k_{ps}^{(b)}$, from Eqs. (32) and (37), respectively, yield

$$K_{\mathrm{eq}}^{ps} = \frac{k_{ps}^{(f)}}{k_{ps}^{(b)}} = \left(\frac{2kT}{D}\right)^{1/2}\frac{\sigma^2[L_c-(4\epsilon_{ps}/kT)^{1/n_1}\Gamma(1-1/n_1)][1-e^{-L^2/4D}]e^{\epsilon_{ps}/kT}}{\epsilon_{ps}^{1/2}n_1 2^{1/2-1/n_1}}. \tag{38}$$

D. Important rate and equilibrium constant ratios

1. Dimerization

From Eqs. (25), (26), and (38) for the concentration equilibrium constants, the following ratio are obtained:

$$\frac{K_{\mathrm{eq12}}^{(2d)}}{K_{\mathrm{eq12}}^{(3d)}} = \frac{1}{2}\frac{\int_\sigma^{\sigma(n\epsilon_1/kT)^{1/n}} dRRe^{(\epsilon_1/kT)(\sigma/R)^n}}{\int_\sigma^{\sigma(n\epsilon_1/2kT)^{1/n}} dRR^2e^{(\epsilon_1/kT)(\sigma/R)^n}}, \tag{39}$$

$$\frac{K_{\mathrm{eq}}^{ps}}{K_{\mathrm{eq12}}^{(3d)}} = \left(\frac{2kT}{D}\right)^{1/2}\frac{\sigma^2\left[L_c-(4\epsilon_{ps}/kT)^{1/n_1}\Gamma\left(1-\frac{1}{n_1}\right)\right][1-e^{-L^2/4D}]e^{\epsilon_{ps}/kT}}{2\pi\epsilon_{ps}^{1/2}n_1 2^{1/2-1/n_1}\int_\sigma^{\sigma(n\epsilon_1/2kT)^{1/2}} dRR^2e^{(\epsilon_1/kT)(\sigma/R)^n}} \tag{40}$$

Using Eq. (4), relating fractional and concentration equilibrium constants, we obtain the fractional equilibrium constant ratios,

$$\frac{\mathrm{Kp}_{12}^{(2d)}}{\mathrm{Kp}_{12}^{(3d)}} = \frac{1}{2}\frac{\int_\sigma^{\sigma(n\epsilon_1/kT)^{1/n}} dRRe^{(\epsilon_1/kT)(\sigma/R)^n}}{\int_\sigma^{\sigma(n\epsilon_1/2kT)^{1/n}} dRR^2e^{(\epsilon_1/kT)(\sigma/R)^n}}L, \tag{41}$$

and

$$\frac{\mathrm{Kp}^{ps}}{\mathrm{Kp}_{12}^{(3d)}} = 2^{1/n_1}\frac{\sigma^2[L_c-(4\epsilon_{ps}/kT)^{1/n_1}\Gamma(1-1/n_1)][1-e^{-L^2/4D}]e^{\epsilon_{ps}/kT}}{2\pi\sqrt{D(\epsilon_{ps}/kT)}n_1\int_\sigma^{\sigma(n\epsilon_1/2kT)^{1/n}} dRR^2e^{\epsilon_1/kT(\sigma/R)^n}}\frac{1}{2L[B]_{\mathrm{tot}}}. \tag{42}$$

Next, some important rate ratios are considered. The rate Rh_{ps} of the monomer-surface aggregation in the high friction limit is given by $k_f^{ps}[B_f]L^2$, as discussed in Sec. III C, where k_f^{ps} is given by Eq. (32). The rate of aggregation of two spherical monomers in solution $(3d)$, is given by

$$\mathrm{Rh}_{2p}^{(3d)} = k_{3d}^{(2)}[B_f]^2L^3, \tag{43}$$

where $k_{3d}^{(2)}$ is given by Eq. (24). Therefore the ratio of the two rates is given by

$$\frac{\mathrm{Rh}_{ps}}{\mathrm{Rh}_{2p}^{(3d)}} = \frac{\sqrt{D}}{D_{\mathrm{eff}}}\frac{[1-e^{-L^2/4D}]\int_\sigma^{\mathrm{Rc}_3} dR(1/R^2)e^{-(\epsilon_1/kT)(\sigma/R)^n}}{2\pi\sqrt{\pi}cL} = \frac{\sqrt{D}}{D_{\mathrm{eff}}}\frac{[1-e^{-L^2/4D}]\int_\sigma^{\mathrm{Rc}_3} dR(1/R^2)e^{-(\epsilon_1/kT)(\sigma/R)^n}}{2\pi\sqrt{\pi}\alpha_f[B]_{\mathrm{tot}}L}. \tag{44}$$

The next ratio to be considered is that of the rates of dimerization on the surface and in solution. This is probably the ratio of greatest interest, at least for comparing association in a volume with association on a surface such as a membrane.

The rate for dimerization on the surface is given by the equation

$$\mathrm{Rh}_{2p}^{(2d)} = k_{2d}^{(2)}[B_i]^2L^2, \tag{45}$$

where $k_{2d}^{(2)}$ is given by Eq. (23). The ratio of $\mathrm{Rh}_{2p}^{(2d)}$ to $\mathrm{Rh}_{2p}^{(3d)}$ [Eq. (43)] is

$$\frac{\mathrm{Rh}_{2p}^{(2d)}}{\mathrm{Rh}_{2p}^{(3d)}} = \frac{1}{2}\frac{\int_\sigma^{\mathrm{Rc}_3} dR(1/R^2)e^{-(\epsilon_1/kT)(\sigma/R)^n}}{\int_\sigma^{\mathrm{Rc}_2} dR(1/R)e^{-(\epsilon_1/kT)(\sigma/R)^n}}(K_{\mathrm{eq}}^{ps})^2\frac{1}{L}. \tag{46}$$

2. Formation of larger aggregates

If the concentration equilibrium constant for formation of an n-mer ($n=2,3,4,\ldots$) from an $(n-1)$-mer in solution is denoted by $K^{(3d)}_{\mathrm{eq}(n-1)n}$, then $[B_{fn}]$ can be expressed as

$$[B_{fn}] = K^{(3d)}_{\mathrm{eq}(n-1)n} K^{(3d)}_{\mathrm{eq}(n-2)(n-1)} \cdots K^{(3d)}_{\mathrm{eq}12} [B_f]^n. \tag{47}$$

The rate of formation of an $(n+1)$-mer from an n-mer in solution is given by

$$\mathrm{Rh}^{(3d)}_{(n+1)p} = k^{(2)}_{3d} [B_{fn}][B_f] L^3. \tag{48}$$

Substituting $[B_{fn}]$ from Eq. (47) in the above equation yields

$$\mathrm{Rh}^{(3d)}_{(n+1)p} = k^{(2)}_{3d} K^{(3d)}_{\mathrm{eq}(n-1)n} K^{(3d)}_{\mathrm{eq}(n-2)(n-1)} \cdots K^{(3d)}_{\mathrm{eq}12} [B_f]^{n+1} L^3. \tag{49}$$

Similarly, the rate for the corresponding surface process is given by

$$\mathrm{Rh}^{(2d)}_{(n+1)p} = k^{(2)}_{2d} K^{(2d)}_{\mathrm{eq}(n-1)n} K^{(2d)}_{\mathrm{eq}(n-2)(n-1)} \cdots K^{(2d)}_{\mathrm{eq}12} \times (K^{ps}_{\mathrm{eq}})^{n+1} [B_f]^{n+1} L^2, \tag{50}$$

where $K^{ps}_{\mathrm{eq}} = [B_i]/[B_f]$.

The ratio of the rate of formation of an $(n+1)$-mer from an n-mer on the surface to the corresponding rate in solution can be obtained by dividing Eq. (50) by Eq. (49) and is given by

$$\frac{\mathrm{Rh}^{(2d)}_{(n+1)p}}{\mathrm{Rh}^{(3d)}_{(n+1)p}} = \frac{k^{(2)}_{2d}}{k^{(2)}_{3d}} \left(\frac{K^{(2d)}_{\mathrm{eq}}}{K^{(3d)}_{\mathrm{eq}}} \right)^{n-1} \frac{(K^{ps}_{\mathrm{eq}})^{n+1}}{L}, \tag{51}$$

which follows from the fact that, in our model,

$$\frac{K^{(2d)}_{\mathrm{eq}12}}{K^{(3d)}_{\mathrm{eq}12}} = \frac{K^{(2d)}_{\mathrm{eq}23}}{K^{(3d)}_{\mathrm{eq}23}} = \cdots = \frac{K^{(2d)}_{\mathrm{eq}(n-1)n}}{K^{(3d)}_{\mathrm{eq}(n-1)n}} = \frac{K^{(2d)}_{\mathrm{eq}}}{K^{(3d)}_{\mathrm{eq}}}. \tag{52}$$

Equation (51) also holds for dimerization, since substituting $n=1$ in that equation reproduces Eq. (46).

In order to plot any of the rate and equilibrium constant ratios in this section, as a function of ϵ_1, ϵ_{ps}, and σ, one needs the expressions for Rc_2 and Rc_3 in terms of these parameters. The mean separations between a monomer and an n-mer on the surface and in solution are denoted by $\mathrm{Rc}^{(1n)}_2$ and $\mathrm{Rc}^{(1n)}_3$, respectively. When A and B are identical it can be inferred from Eq. (10) of supplementary information[7] that

$$[B_i] = \frac{1}{\pi (\mathrm{Rc}^{(11)}_2)^2}. \tag{53}$$

Similarly, for the three-dimensional case, it can be shown that

$$[B_f] = \frac{1}{4\pi (\mathrm{Rc}^{(11)}_3)^3/3}. \tag{54}$$

The above equations yield the following expressions for Rc_2 and Rc_3:

$$\mathrm{Rc}^{(11)}_2 = \left(\frac{1}{\pi \alpha_f K^{ps}_{\mathrm{eq}} [B]_{\mathrm{tot}}} \right)^{1/2} \tag{55}$$

$$\mathrm{Rc}^{(11)}_3 = \left(\frac{3}{4\pi \alpha_f [B]_{\mathrm{tot}}} \right)^{1/3}. \tag{56}$$

Similarly,

$$\mathrm{Rc}^{(12)}_2 = \left(\frac{1}{\pi (K^{(2d)}_{\mathrm{eq}12} (K^{ps}_{\mathrm{eq}} \alpha_f [B]_{\mathrm{tot}})^3)^{1/2}} \right)^{1/2}, \tag{57}$$

$$\mathrm{Rc}^{(12)}_3 = \left(\frac{3}{4\pi (K^{(3d)}_{\mathrm{eq}12} (\alpha_f [B]_{\mathrm{tot}})^3)^{1/2}} \right)^{1/3}, \tag{58}$$

$$\mathrm{Rc}^{(13)}_2 = \left(\frac{1}{\pi (K^{(2d)}_{\mathrm{eq}12} K^{(2d)}_{\mathrm{eq}23} (K^{ps}_{\mathrm{eq}} \alpha_f [B]_{\mathrm{tot}})^4)^{1/2}} \right)^{1/2}, \tag{59}$$

$$\mathrm{Rc}^{(13)}_3 = \left(\frac{3}{4\pi (K^{(3d)}_{\mathrm{eq}12} K^{(3d)}_{\mathrm{eq}12} (\alpha_f [B]_{\mathrm{tot}})^4)^{1/2}} \right)^{1/3}. \tag{60}$$

It is fairly straightforward to obtain from the above equations the different Rc_2 and Rc_3 expressions in terms of ϵ_1, ϵ_{ps}, and σ.

IV. RESULTS AND DISCUSSION

For the specific case in which the largest possible aggregate is that of four monomers, we calculate the rate and equilibrium constant ratios in Sec. III D as a function of three parameters, viz., intermonomer binding energy (ϵ_1), monomer-surface binding energy (ϵ_{ps}), and monomer size (σ). Our main focus is on investigating the conditions under which one rate or equilibrium constant dominates over another, as one scans different regions of the parameter space. This is achieved by varying two parameters at a time, and obtaining binary contour diagrams of the logarithm, to the base ten, of the ratio of two rates or equilibrium constants as a function of the two varied parameters. In these binary plots, a single contour line divides the positive values of the logarithm (ratio >1) from the negative values (ratio <1). The positive and negative regions in the binary plots are colored white and black, respectively. These plots efficiently point out the parameter regimes in which one rate or equilibrium constant dominates over another, thereby specifying the manner in which one or more parameters should be tuned to favor one rate or equilibrium constant over another.

A. Choice of parameters

In order to quantify the variation of the relevant ratios with the three parameters, some feasible numerical values are assigned to characterize the model. The box size L is taken as 1 cm. The total number of monomers present in all the different forms is taken to be 6.022×10^{11}, so that the total concentration of the monomers $[B]_{\mathrm{tot}}$ in the system is 1 nM which is of the order of *in vivo* concentration of amyloid fragments in the cerebrospinal fluid of the human brain.

The potential well is considered to extend up to $L_c\sigma$, where $L_c=10$ and σ is the diameter of the monomer. In calculating the diffusion coefficient, the viscosity coefficient of water at 20 °C, 1.002×10^{-3} kg m^{-1} s^{-1}, is used. Then, for the length of the cubic box $L=1$ cm, and for the range of monomer size considered, the value of $[1-e^{-L^2/4D}]$ in the

expression for $k_{ps}^{(f)}$ in Eq. (32) can be taken as 1 for all practical purposes. The binding energies are specified in units of kT and the monomer diameter in angstroms. The intermonomer and monomer-surface binding energies are represented as ϵ_1/kT and ϵ_{ps}/kT, respectively, and the monomer diameter as σ/Å. Henceforth, for convenience, ϵ_{ps}/kT and ϵ_1/kT are referred to as ϵ_{ps} and ϵ_1, respectively. The lowest value of ϵ_{ps}/kT we allow is 10, so that both inequalities (35) and (36) are satisfied for $L_c=10$, as discussed in Sec. III C. The value of ϵ_{ps} is varied in the range of $10kT-100kT$.

Our model does not account for any repulsion between a monomer approaching the surface and the adsorbed monomers that would reduce the available area of the surface. Hence, its results are meaningful only for parameter regimes in which the surface is far from saturation, i.e., the mean separation between the monomers on the surface is much larger than the contact distance of two monomers. The largest value of the molecular size parameter σ that we consider is 100 Å. This is of the order of the radius of gyration of some large biomolecules. Besides, for this upper bound of σ, the mean separation between two monomers on the surface is at least six times the contact distance between two monomers, even if the lowest value ($8kT$) of intermonomer binding energy (ϵ_1) in our model is considered. (Lowest ϵ_1 value corresponds to the maximum possible number of monomers on the surface.)

All the calculations and plotting are done using MATHEMATICA version 5.2.

B. Ratio of adsorption rate to solution dimerization rate

The first ratio to be considered is the ratio of the rate of monomer adsorption to the rate of dimerization in solution, $\mathrm{Rh}_{ps}/\mathrm{Rh}_{2p}^{(3d)}$, denoted by the shorthand notation r_{w3d}. A binary plot of $\log(r_{w3d})$ plotted as a function of ϵ_1 and ϵ_{ps}, keeping σ fixed at 100 Å [Fig. 1(a)] clearly shows that r_{w3d} increases with both ϵ_1 and ϵ_{ps}. Similar plots, for other fixed σ values, exhibit larger negative (black) region for smaller fixed σ values, thereby implying that r_{w3d} is an increasing function of σ as well. This is validated by the binary diagram of $\log(r_{w3d})$ as a function of ϵ_1 and σ [Fig. 1(b)].

As shown by Eq. (24), increasing the intermonomer binding energy ϵ_1 increases the second order solution dimerization rate coefficient $[k_2^{(3d)}]$. Physically, this relates the increase in the total cross section for dimerization with increase in the binding energy between the monomers. On the other hand, increasing ϵ_1 has no effect on the rate constant for adsorption of a monomer $[k_{ps}^{(f)}]$, as shown by Eq. (32), because the monomers in solution and on the surface are equally affected by increasing ϵ_1. Hence, the ratio of the adsorption rate constant to the dimerization rate coefficient $[k_{ps}^{(f)}/k_2^{(3d)}]$ decreases with increasing ϵ_1.

The only effect of increasing monomer-surface binding energy ϵ_{ps} on the solution dimerization rate coefficient is to increase the intermonomer separation in solution, $\mathrm{Rc}_3^{(11)}$. Increasing ϵ_{ps} reduces the number of monomers in solution, leading to an increase in $\mathrm{Rc}_3^{(11)}$. As is evident from Eq. (22), a larger $\mathrm{Rc}_3^{(11)}$ implies a smaller crossing frequency $\omega_T^{(3d)}$ of

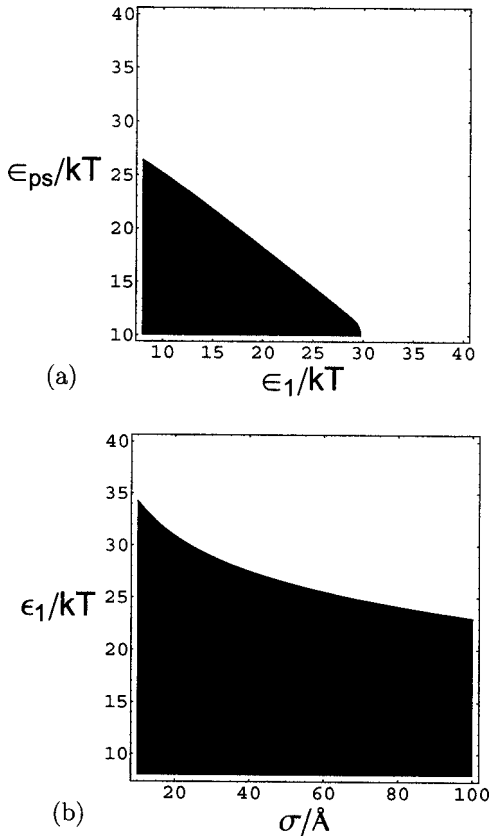

FIG. 1. Binary diagrams of $\log_{10}$(monomer adsorption rate/solution dimerization rate). (a) The horizontal and vertical axes represent intermonomer binding energy and monomer-surface binding energy, respectively; monomer diameter (σ) is fixed at 100 Å. (b) Horizontal and vertical axes represent monomer diameter and intermonomer binding energy, respectively; monomer-surface binding energy is fixed at $16kT$.

the effective association barrier in solution, and hence, a lower solution dimerization rate coefficient. However, this effect of increasing ϵ_{ps} on the solution dimerization rate coefficient $k_2^{(3d)}$ turns out to be negligible. Neither does an increase in ϵ_{ps} influence the adsorption rate constant, as shown by Eq. (32), because the rate at which the monomer gets adsorbed at the surface is diffusion limited. Hence, the variation of ϵ_{ps} slightly increases the ratio of the adsorption rate constant to the solution dimerization rate coefficient.

However, higher values of both binding energies ϵ_1 and ϵ_{ps} lead to a lower concentration of monomers in solution which lowers both the dimerization and adsorption rates. With decreasing monomer concentration in solution, it becomes more difficult for a monomer to find another monomer than for a monomer to find the surface, leading to the dimerization rate being lowered more than the adsorption rate. This explains the increasing trend of r_{w3d} with ϵ_{ps} as both the rate coefficient part and the concentration part of r_{w3d} increase with ϵ_{ps}. Increasing ϵ_1 has both increasing (concentration part) and decreasing effects (rate coefficient part) on r_{w3d}. The dominance of the incremental over the decremental effect causes the overall increase of r_{w3d} with ϵ_1.

From Eq. (32), it follows that the adsorption rate constant decreases with increasing σ as the diffusion coefficient decreases with the monomer size (Stokes-Einstein relation). The increase in the solution dimerization rate coefficient

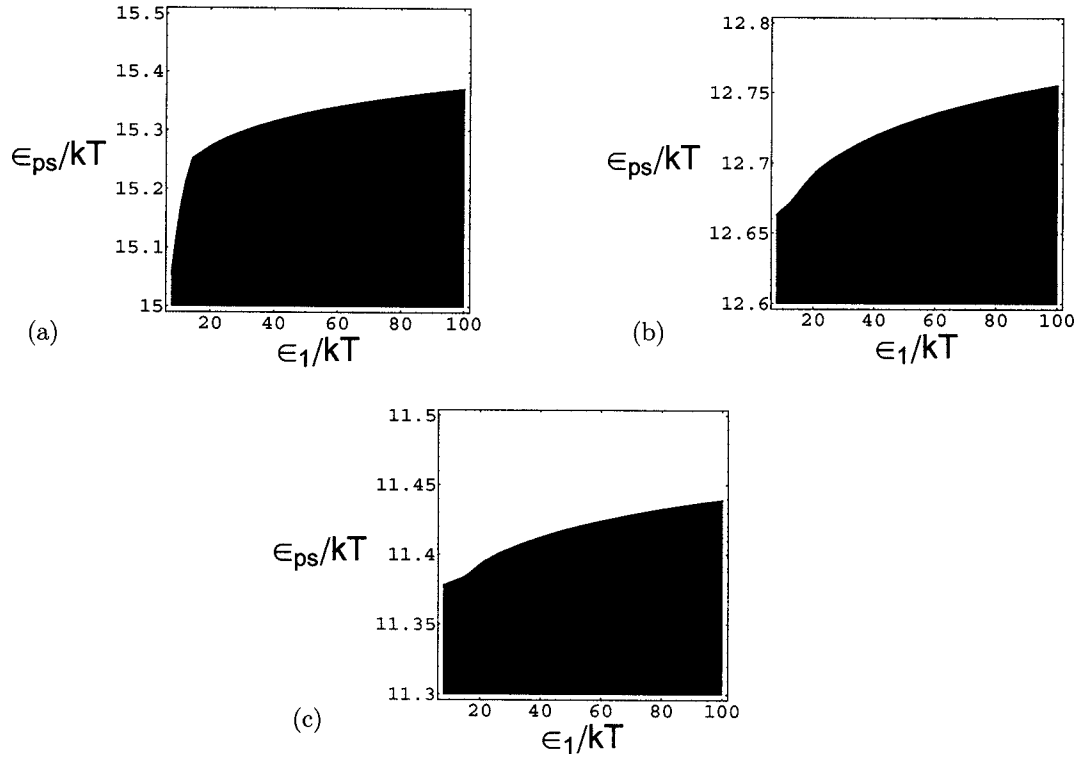

FIG. 2. Binary diagrams of (a) $\log_{10}$(surface dimerization rate/solution dimerization rate), (b) $\log_{10}$(surface trimer formation rate/solution trimer formation rate), and (c) $\log_{10}$(surface tetramer formation rate/solution tetramer formation rate) for monomer diameter (σ) of 100 Å. The horizontal and vertical axes represent intermonomer binding energy and monomer-surface binding energy, respectively.

with σ, as indicated by Eq. (24), can be traced to an increase in the crossing frequency $\omega_T^{(3d)}$ [Eq. (22)] of the effective one-dimensional association barrier in solution. Therefore, the ratio of the adsorption rate constant to the solution dimerization rate coefficient decreases with increasing σ. However, increasing the monomer size (diameter) leads to more frequent encounters between monomers, thereby reducing the equilibrium concentration of monomers in solution. The lowering in concentration of monomers in solution reduces the dimerization rate $[\mathrm{Rh}_{2p}^{(3d)}]$ more than the adsorption rate (Rh_{ps}), as explained in the previous paragraph. Thus, the concentration part of r_{w3d} increases with σ and this effect dominates the decremental influence on the rate coefficient part with increasing σ, leading to the overall increasing trend.

C. Ratio of surface versus solution dimerization rates

The ratio of the surface dimerization rate to the corresponding solution dimerization rate, $\mathrm{Rh}_{2p}^{(2d)}/\mathrm{Rh}_{2p}^{(3d)}$, is denoted by the shorthand notation $r_{1\to 2}$. A binary contour plot of $\log(r_{1\to 2})$ as a function of ϵ_1 and ϵ_{ps} [Fig. 2(a)], with $\sigma = 100$ Å, reveals that $r_{1\to 2}$ increases with ϵ_{ps} and decreases with ϵ_1. A binary plot of $\log(r_{1\to 2})$ as a function of ϵ_1 and σ [Fig. 3(a)] implies that $r_{1\to 2}$ is an increasing function of σ.

As shown by Eq. (46), the concentration part of $r_{1\to 2}$ varies as the square of the adsorption equilibrium constant K_{eq}^{ps}, which increases with ϵ_{ps}, as shown by Eq. (38). Physically, the higher the ratio of the number of surface to solution monomers, the more favored is dimerization at the surface over that in solution.

The ratio of the total association cross section at the surface to that in solution $[k_2^{(2d)}/k_2^{(3d)}]$ also increases with increasing ϵ_{ps}. Increasing ϵ_{ps} decreases the number of single monomers in solution and increases the number of single monomers on the surface, thereby increasing the mean intermonomer separation $\mathrm{Rc}_3^{(11)}$ in solution and decreasing the mean intermonomer separation $\mathrm{Rc}_2^{(11)}$ on the surface. Physi-

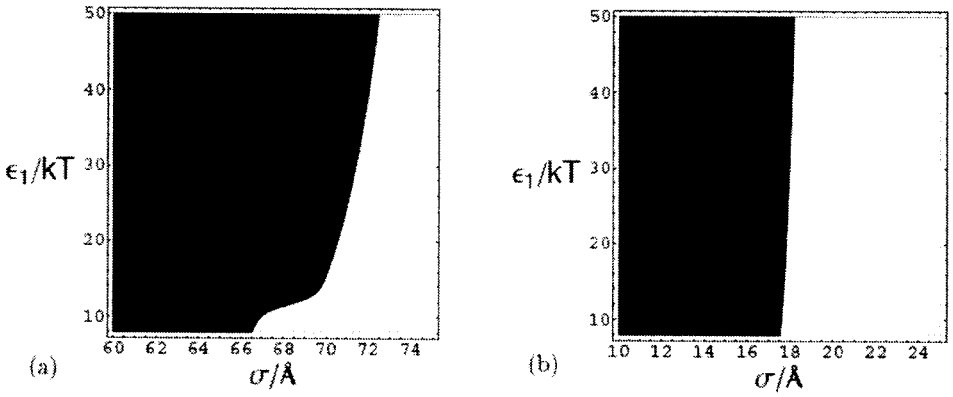

FIG. 3. Binary diagrams of (a) $\log_{10}$(surface dimerization rate/solution dimerization rate) and (b) $\log_{10}$(surface trimer formation rate/solution trimer formation rate) for monomer-surface binding energy of $16kT$. The horizontal and the vertical axes represent monomer diameter and intermonomer binding energy, respectively.

cally, the effective barrier crossing frequency $\omega_T^{(2d)}$ [Eq. (21)] at the surface is enhanced due to the increase in concentration of monomers on the surface, which results from increased ϵ_{ps}. Lowering the concentration of monomers in solution similarly leads to a decrease in the barrier crossing frequency in the solution case $\omega_T^{(3d)}$ [Eq. (22)]. The overall effect is the increase of ratio of surface versus solution dimerization rate coefficients with ϵ_{ps}. It should be pointed out that this effect is much smaller in magnitude than that of increasing ϵ_{ps} on the concentration part of $r_{1\to 2}$.

The ϵ_1 dependence of $r_{1\to 2}$ is the ϵ_1 dependence of the corresponding second order rate coefficients, as the concentration-dependent part of $r_{1\to 2}$, $(K_{\mathrm{eq}}^{ps})^2/L$, is independent of ϵ_1 as shown by Eqs. (46) and (38). The second order rate coefficient for dimerization at the surface $[k_2^{(2d)}]$ decreases with ϵ_1, whereas that for dimerization in solution $[k_2^{(3d)}]$ increases with ϵ_1. This causes $r_{1\to 2}$ to decrease with increasing ϵ_1. Increasing ϵ_1 lowers the effective association barrier, thereby enhancing the barrier crossing frequencies $\omega_T^{(2d)}$ and $\omega_T^{(3d)}$, as is evident from Eqs. (21) and (22), respectively. At the same time, increasing ϵ_1 also reduces the number of single monomers on the surface and in solution, thereby increasing $\mathrm{Rc}_2^{(11)}$ and $\mathrm{Rc}_3^{(11)}$, as a result of which, the barrier crossing frequencies $\omega_T^{(2d)}$ and $\omega_T^{(3d)}$ are reduced. For surface dimerization, the decremental effect of increasing ϵ_1 on the barrier crossing frequency overcomes the incremental effect. However, for dimerization in solution, the situation is just the opposite, because the rate at which $\mathrm{Rc}_3^{(11)}$ increases with ϵ_1 is slower than the rate of increase of $\mathrm{Rc}_2^{(11)}$ with ϵ_1. Physically, by virtue of the lower dimensionality of the surface compared to the solution, increasing ϵ_1 reduces the concentration of monomers and, hence, increases the mean monomer separation on the surface more rapidly than in solution. Thus, the decremental effect of increasing ϵ_1 on the effective barrier crossing frequency $\omega_T^{(3d)}$ in solution is overcome by the incremental effect of increasing ϵ_1 on $\omega_T^{(3d)}$ [Eq. (22)].

The concentration part of the rate ratio $r_{1\to 2}$ varies as the square of K_{eq}^{ps} which can be shown to vary as $\sigma^{2.5}$ [Eq. (38)]and hence increases with increasing σ. Increasing σ reduces the concentration of monomers in solution, as well on the surface, because increasing monomer size leads to more frequent encounters of monomers with each other. The effect of increasing σ is more pronounced in the solution case relative to the surface case because the effect is felt in three dimensions in the former case and in two dimensions in the latter. The rate coefficient for escape of a monomer from the the surface $[k_{ps}^{(b)}]$ is also lowered by increasing σ, as is evident from Eq. (37). Hence, with increasing σ, the monomer concentration on the surface drops more slowly than the corresponding solution concentration. Moreover, for low values of the binding energies, e.g., $\epsilon_1=10kT$ and $\epsilon_{ps}=16kT$, the increase in the number of monomers on the surface, with increasing σ, is greater than the increment in the number of surface monomers that aggregate. Thus, depending on the binding energy values, increasing σ leads either to slower depletion of monomers on the surface than in solution or to an actual increase of surface monomer concentration. These trends of variation of the surface and solution monomer concentrations lead to the increase of K_{eq}^{ps} with increasing σ.

Both the surface and solution second order rate coefficients $k_2^{(2d)}$ and $k_2^{(3d)}$ increase with σ because increasing σ raises the barrier crossing frequency ω_T in both the surface and solution cases [Eqs. (21) and (22)]. However, the effective barrier crossing frequency in solution, $\omega_T^{(3d)}$, is boosted more than that at the surface, $\omega_T^{(2d)}$, with increasing σ, because in the surface case, the size increase is felt in two dimensions, whereas it is also felt in an additional third dimension in the solution case. Therefore, the ratio $k_2^{(2d)}/k_2^{(3d)}$ decreases with σ. Though the ratio of the surface to solution rate coefficients decreases with increasing σ, the concentration part of the rate ratio increases with σ, leading to an overall increase of the rate ratio with σ.

D. Rates of surface versus solution rates for formation of larger aggregates

Next, we consider the corresponding rate ratios for formation of trimers from dimers ($r_{2\to 3}$) and formation of tetramers from trimers ($r_{3\to 4}$). Comparison of binary contour plots of $r_{2\to 3}$ and $r_{3\to 4}$ as functions of ϵ_1 and ϵ_{ps}, for monomer diameter of 100 Å [Figs. 2(b) and 2(c)], with the corresponding dimerization plot [Fig. 2(a)] shows that the larger the aggregate formed, the lower are the values of the monomer-surface binding energy ϵ_{ps} at which crossover from faster solution association to faster surface association becomes possible. Comparison of binary plots of $r_{2\to 3}$, as functions of ϵ_1 and σ [Fig. 3(b) with the corresponding dimerization plot, Fig. 3(a)] also shows that the crossover from faster solution association to faster surface association occurs at lower σ values for higher degrees of association. Thus, the higher the degree of association, the stronger is the dependence of $r_{n\to(n+1)}$ $(n=2,3,4,\ldots)$ on ϵ_{ps} and σ.

The rate coefficient ratio in Eq. (51), $k_2^{(2d)}/k_2^{(3d)}$, increases with increasing ϵ_{ps}, as has already been explained in Sec. IV C. Equations (25) and (26) show that the ratio $K_{\mathrm{eq}}^{(2d)}/K_{\mathrm{eq}}^{(3d)}$ in Eq. (51) is independent of ϵ_{ps}. The ratio $r_{n\to(n+1)}$ varies as the $(n+1)$th power of the adsorption-desorption equilibrium constant K_{eq}^{ps}, which has a dominant exponential dependence on ϵ_{ps}. This explains the monotonically increasing trend of $\log(r_{n\to(n+1)})$ with ϵ_{ps}. The larger the value of n, the stronger is the dependence of K_{eq}^{ps}, and hence of $r_{n\to(n+1)}$, on ϵ_{ps}. An increase in ϵ_{ps} increases the ratio of surface bound to solution aggregates more than the ratio of surface bound to solution monomers, because the effect of the surface on the aggregate, comprising of a number of monomers, is greater than that on a single monomer. Hence, the larger the aggregate size (n), the greater is the increase in the ratio of the surface versus solution association rates for a given increase in ϵ_{ps}.

As has been discussed previously in Sec. IV C, the ratio of the second order association rate coefficients for dimerization decreases with σ. The ratio of association equilibrium constants $(K_{\mathrm{eq}}^{(2d)}/K_{\mathrm{eq}}^{(3d)})$ also decreases with σ, as will be shown later in Sec. IV F. On the other hand, the ratio of the surface to solution concentrations of monomers (K_{eq}^{ps}), and hence of aggregates, increases with σ, as is evident from

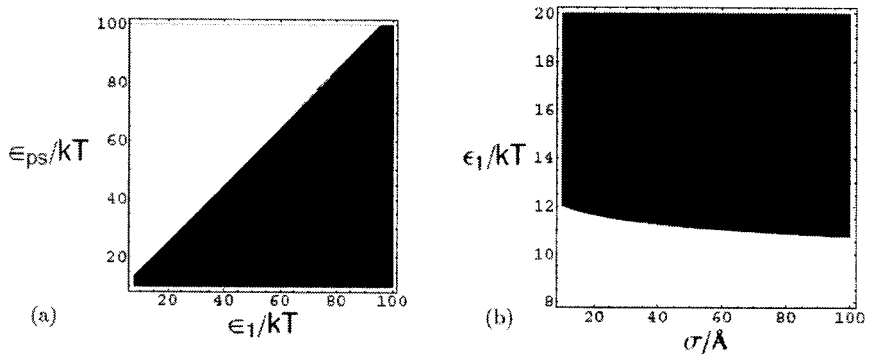

FIG. 4. Binary diagrams of $\log_{10}$(monomer adsorption-desorption equilibrium constant/solution dimerization equilibrium constant); (a) Horizontal and vertical axes are intermolecular binding energy and monomer-surface binding energy; monomer diameter is 100 Å; (b) Horizontal and vertical axes are monomer diameter and intermonomer binding energy; surface binding energy is $16kT$.

Eq. (38). Of these two opposing effects, the incremental effect dominates and this dominance increases with the degree of association, as shown by Eq. (51).

The rate of increase of the ratio of surface versus solution aggregate concentrations with σ is faster than that for monomers. As the monomer size is increased, the concomitant size increase of the aggregate is even greater because of the cumulative effect of the increase in size of the constituent monomers. As a result, the adsorption-desorption equilibrium for the aggregates is pushed more towards adsorption, relative to that for the monomers, by suppressing the desorption process, as is evident from Eq. (37). This causes the crossover from a faster solution to a faster surface association rate at lower values of σ than in the dimerization case.

E. Ratio of adsorption equilibrium constant to solution dimerization equilibrium constant

The ratio $\mathrm{Kp}_{\mathrm{eq}}^{ps}/\mathrm{Kp}_{12}^{(3d)}$ is denoted by the shorthand notation χ_{w3d}. Binary plots of $\log(\chi_{w3d})$ as a function of ϵ_1 and ϵ_{ps}, for a range of fixed monomer sizes, imply that χ_{w3d} increases with ϵ_{ps} and decreases with ϵ_1 [Fig. 4(a)]. A binary diagram of $\log(\chi_{w3d})$ with varying ϵ_1 and σ, keeping ϵ_{ps} fixed at 16 [Fig. 4(b)], shows that χ_{w3d} is a decreasing function of σ, and the variation of χ_{w3d} with σ is much less pronounced than with the other two parameters.

As mentioned earlier in Sec. IV C, the adsorption-desorption equilibrium constant K_{eq}^{ps} and hence Kp^{ps} is independent of ϵ_1. Increasing ϵ_1 increases the dimerization equilibrium constant $K_{\mathrm{eq12}}^{(3d)}$, as shown by Eq. (26), and hence $\mathrm{Kp}_{12}^{(3d)}$. This causes the ratio χ_{w3d} to decrease with increasing ϵ_1.

As explained earlier in Sec. IV C, K_{eq}^{ps} and hence Kp^{ps} increases with ϵ_{ps}. Since our model does not distinguish between ϵ_{ps} for an isolated monomer from that for a constituent monomer in an aggregate, the solution dimerization equilibrium constant is independent of ϵ_{ps}, as shown by Eq. (26). These differing trends of variation in Kp^{ps} and $\mathrm{Kp}_{12}^{(3d)}$ with ϵ_{ps} cause the ratio χ_{w3d} to increase with increasing ϵ_{ps}.

As shown by Eqs. (38) and (26), both the adsorption and the solution dimerization equilibrium constants increase with σ. In the dimerization equilibrium, both the reacting monomers are influenced by increasing σ, whereas in the adsorption equilibrium, the surface is unaffected and only the monomer is influenced by an increasing σ. Hence, the rate of increase of the dimerization equilibrium constant with σ is greater than that of the adsorption equilibrium constant, leading to an overall decrease of $\log(\chi_{w3d})$ with increasing σ.

F. Ratio of surface versus solution association equilibrium constants

Our theoretical model does not consider any connection of the intermonomer binding energy ϵ_1, with the monomer-surface interaction energy ϵ_{ps}, so that ϵ_1 in solution is the same as that on surface. Therefore, the ratio $K_{\mathrm{eq12}}^{(2d)}/K_{\mathrm{eq12}}^{(3d)}$, and hence $\mathrm{Kp}_{12}^{(2d)}/\mathrm{Kp}_{12}^{(3d)}$ (denoted by χ_{2d3d}), which varies with ϵ_1, is independent of ϵ_{ps}, as shown by Eqs. (25) and (26).

A contour plot of $\log(\chi_{2d3d})$ shows that $\log(\chi_{2d3d})$ is always positive for the range of σ and ϵ_1 considered. Comparison of the plots of $\log(\chi_{2d3d})$ varying individually with σ and ϵ_1, in Figs. 5(a) and 5(b), respectively, shows that the variation of $\log(\chi_{2d3d})$ with σ is much more pronounced than that

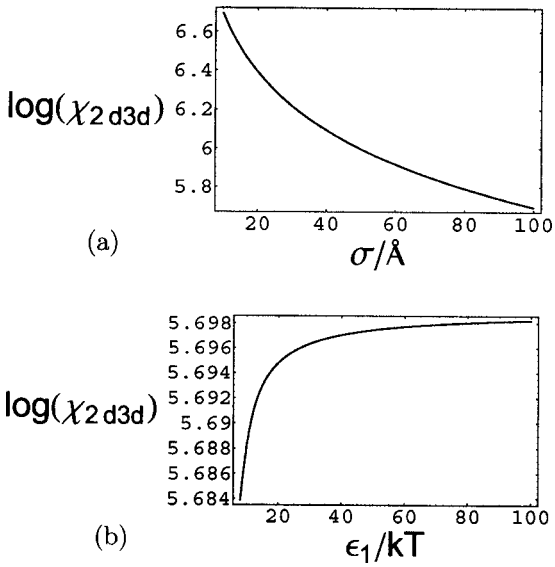

FIG. 5. Plots of $\log_{10}$(surface dimerization equilibrium constant/solution dimerization equilibrium constant) (a) vs monomer diameter for intermonomer binding energy of $20kT$ and (b) vs intermonomer binding energy for monomer diameter of 100 Å.

with ϵ_1, resulting from the stronger dependence on σ than on ϵ_1 of both the equilibrium constants, $K_{eq12}^{(2d)}$ and $K_{eq12}^{(3d)}$, as evident from Eqs. (25) and (26).

Figure 5(b) shows the variation of $\log(\chi_{2d3d})$ with ϵ_1 for a monomer diameter of 100 Å. On varying ϵ_1, $\log(\chi_{2d3d})$ increases monotonically with ϵ_1, finally approaching a constant value asymptotically. Comparison with the plots at other σ values shows that the final asymptotic value of $\log(\chi_{2d3d})$ decreases with the monomer size. This decreasing trend of χ_{2d3d} with increasing σ is corroborated by Fig. 5(a).

Equations (25) and (26) show that both the surface and solution dimerization constants increase with ϵ_1. The surface equilibrium constant $K_{eq12}^{(2d)}$ increases more rapidly with ϵ_1 than the solution constant $K_{eq12}^{(3d)}$, leading to an increasing trend of $\log(\chi_{2d3d})$ with ϵ_1. This physically interprets as a greater increase in the dimer (n-mer) concentration on the surface than in solution, with increasing ϵ_1. Because the surface has one dimension less than the solution, the effect of increasing the ϵ_1 on the dimer (n-mer) concentration is more pronounced on the surface than in solution.

Both the surface and solution equilibrium constants increase with σ, as shown by Eqs. (25) and (26). The effect is more pronounced for the solution case because it is felt only in two dimensions in the surface case and in three dimensions in solution. This causes the ratio of the two equilibrium constants and, hence, its logarithm to decrease with increasing σ.

G. Scope of the model

The results obtained in this article should apply to systems whose constituent monomers can be approximated as spheres interacting with each other and with any nearby extended surface, primarily through dispersion interactions. Hence, it is worthwhile to try applying these results to model the formation of short chainlike aggregates of globular biomolecules suspended in a cellular fluid in the proximity of a cellular surface, provided that the interactions between the globular molecules and that between each molecule and the surface are dominated by attractive dispersion interactions. With the appropriate set of parameters, these results might be used to compare between interfacial and solution phase association of globular proteins both from kinetic and thermodynamic viewpoints.

Aggregation of β-amyloid protein fragments leads to formation of amyloid plaques commonly found between nerve cells in a human brain affected by Alzheimer's disease. The concentration of the β-amyloid fragments in the cerebrospinal fluid surrounding the nerve cells is very low [2–4 nM (Refs. 16 and 17)] in Alzheimer's patients, as well as in healthy human beings. Hence, it is an interesting question to determine how these aggregates form in spite of this very low concentration. It is highly plausible that the cell surfaces play some role in the aggregation. We suggest that it is possible to use our model as a starting point for learning, from theory, the possible role of cellular surfaces in amyloid plaque formation. In that case, further refinements to our model would be appropriate to take into account the nonspherical shape of the β-amyloid fragments and the role of electrostatics in the aggregation of these fragments.

V. SUMMARY AND CONCLUSIONS

This is a study of the competition between bulk and surface aggregation of monomers in a dense fluid with a surface boundary. We have considered both equilibrium conditions and the kinetics of aggregation, as we examined the relative importance of bulk solution and of surface as sites for aggregation. Several variables play significant roles in this phenomenon. In this article, we have examined this competition by varying three key three parameters: the intermonomer binding energy, the monomer-surface binding energy, and size of the monomers. The calculations show how the rates of binary aggregation and the equilibrium ratios of monomers in solution and on the surface compete and how one or the other can be made to dominate in the high friction regime. The analysis was extended to the binary association rates of monomers with already-formed dimers and larger aggregates, on the surface and in solution. Either of the adsorption-desorption and solution dimerization equilibrium constants may be made to dominate the other by adjusting the same three parameters. One generalization emerges: the surface equilibrium constant for dimer concentration is always greater than the corresponding solution constant for the physically relevant parameter ranges.

Finally, we point out that these results would be a good starting point for comparing the kinetics and thermodynamics of aggregation of globular proteins in solution with that on membranes. In fact, it was just this question that stimulated this study. It was apparent that, to make headway in answering the question of behavior in an organism, one would first have to have a relatively simple model with which to grasp the basic issues of the solution-versus-surface competition.

ACKNOWLEDGMENTS

The authors thank Dr. K. Freed, Dr. A.R. Dinner, Dr. S.C. Meredith, and Dr. Adrienne Boire, for helpful suggestions. This research was supported by a Grant from the National Science Foundation.

APPENDIX A: FAST-PASSAGE TIMES

The first passage time distribution for a monomer starting at $z=0$ at time $t=0$ to arrive at $z=\xi$ has the initial condition $p(z=0,0)=\delta(z=0)$ and the absorbing boundary condition $p(\xi,t)=0$, where $p(z,t)$ is the probability of finding the monomer at z at time t. This probability is obtained by solving the diffusion equation,

$$\frac{\partial p(z,t)}{\partial t} = D\frac{\partial^2 p(z,t)}{\partial z^2}, \tag{A1}$$

subject to the above-mentioned initial and boundary conditions, where D is the diffusion coefficient of the monomer in the continuum liquid. The solution of the above differential equation with the given boundary conditions is given by[18]

$$p(z,t) = \frac{1}{\sqrt{4\pi Dt}}[e^{-z^2/4Dt} - e^{-(2\xi - z)^2/4Dt}]. \quad \text{(A2)}$$

Consequently, the probability that the monomer has not yet reached ξ up to time t is given by

$$R(\xi,t) = \int_{-\infty}^{\xi} dzp(z,t). \quad \text{(A3)}$$

This expression can be written as

$$R(\xi,t) = \frac{2}{\sqrt{\pi}}\int_{0}^{\xi/\sqrt{4Dt}} due^{-u^2}. \quad \text{(A4)}$$

The first passage time density is the negative derivative of R with respect to t.[18] Taking this derivative yields the first passage time distribution in Eq. (31).

APPENDIX B: MONOMER-SURFACE INTERACTION

The potential for interaction between a monomer and an infinitely extended flat surface comprising of ρ monomers per unit area is given by[19]

$$V(z) = (2\pi\rho)4\epsilon_{ps}\left[\left(\frac{\sigma}{z}\right)^{2n_1}\frac{z^2}{2(n_1-1)} - \left(\frac{\sigma}{z}\right)^{n_1}\frac{z^2}{(n_1-2)}\right], \quad \text{(B1)}$$

given that the intermonomer interaction potential has a generalized Lennard-Jones form. A value of $n_1=6$ (corresponding to dispersion interaction between monomers) in Eq. (B1) yields a z^{-10} dependence of the repulsive term and a z^{-4} dependence of the attractive term in the monomer-surface potential. In spite of the fact that $V(z)$ in Eq. (B1) does not reduce to a generalized Lennard-Jones form, it is a reasonable approximation to assume a generalized Lennard-Jones form for monomer-surface potential which retains the z^{-4} dependence of the attractive term of $V(z)$ in Eq. (B1). The generalized Lennard-Jones form of the monomer-surface interaction is much more tractable mathematically, and Larson and Lightfoot[15] have developed a theory of thermally activated escape from a potential well with a generalized Lennard-Jones form.

[1] L.-P. Choo-Smith, W. Garzon-Rodrigues, C. G. Glabe, and W. K. Surewicz, J. Biol. Chem. **272**, 22987 (1997).
[2] V. Koppaka and P. H. Axelsen, Biochemistry **39**, 10011 (2000).
[3] K. Lin, J. C. Crocker, V. Prasad, A. Schofield, D. A. Weitz, T. C. Lubensky, and A. G. Yodh, Phys. Rev. Lett. **85**, 1770 (2000).
[4] D. Letellier and V. Cabuil, Prog. Colloid Polym. Sci. **118**, 248 (2001).
[5] M. Bokvist, F. Lindström, A. Watts, and G. Gröbner, J. Mol. Biol. **335**, 1039 (2004).
[6] J. O. Hirschfelder, C. F. Curtiss, and R. B. Bird, *Molecular Theory of Gases and Liquids* (Wiley, New York, 1954).
[7] See EPAPS Document No. E-JCPSA6-127-505735 for the kinetic derivations described following Eq. (15), for the derivations of Eqs. (25) and (26), and for the full discussion of the low-friction regime. This document can be reached through a direct link in the online article's HTML reference section or via the EPAPS homepage (http://www.aip.org/pubservs/epaps.html).
[8] P. M. Rodger and M. G. Sceats, J. Chem. Phys. **83**, 3358 (1985).
[9] M. G. Sceats, Adv. Chem. Phys. **70**, 357 (1988).
[10] J. M. Dawes and M. G. Sceats, J. Chem. Phys. **88**, 5489 (1988).
[11] H. A. Kramers, Physica (Amsterdam) **7**, 284 (1940).
[12] P. Hänggi, P. Talkner, and M. Borkovec, Rev. Mod. Phys. **62**, 251 (1990).
[13] N. J. Cotes and M. G. Sceats, J. Chem. Phys. **89**, 2816 (1988).
[14] S. A. Allison, C. Chen, and D. Stigler, Biophys. J. **81**, 2558 (2001).
[15] R. S. Larson and E. J. Lightfoot, Physica A **149**, 296 (1988).
[16] R. Motter, C. Vigo-Pelfrey, D. Kholodenko, Ann. Neurol. **38**, 643 (1995).
[17] W. A. van Gool, G. J. Walstra, P. A. Bolhuis, M. A. Kuiper, and E. C. Wolters, Ann. Neurol. **37**, 277 (1995).
[18] R. M. Mazo, *Brownian Motion Fluctuation, Dynamics and Applications* (Clarendon, Oxford, 2002).
[19] J. N. Israelachvili, *Intermolecular and Surface Forces* (Academic, New York, 1985).